Heliyon

ELSEVIER

Received:
14 October 2018
Revised:
29 December 2018
Accepted:
19 March 2019

Cite as: F. Fateminasab, A. K. Bordbar, S. Shityakov. Detailed chemical characterization and molecular modeling of serotonin inclusion complex with unmodified β-cyclodextrin. Heliyon 5 (2019) e01405. doi: 10.1016/j.heliyon.2019.e01405

Detailed chemical characterization and molecular modeling of serotonin inclusion complex with unmodified β-cyclodextrin

F. Fateminasab [a], **A. K. Bordbar** [a,*], **S. Shityakov** [b]

[a] *Department of Chemistry, University of Isfahan, Isfahan, 8174673441, Iran*

[b] *Department of Anesthesia and Critical Care, University of Wurzburg, 97080, Wurzburg, Germany*

[*] Corresponding author.

E-mail addresses: akbordbar@gmail.com, bordbar@chem.ui.ac.ir (A.K. Bordbar).

Abstract

In this study, we analyzed the capability of unmodified β-cyclodextrin (β-CD) to form the stable complex with serotonin hydrochloride (SER), as an important neurotransmitter in the brain. The stable β-CD: SER formulation was prepared and characterized using spectroscopic, thermal, molecular docking, and molecular dynamics techniques, revealing the phenomenon of H-bond formations and the domination of hydrophobic forces between the host molecule and its guest via the amine group of SER and the narrow side of β-CD. The complexation mechanism was mainly enthalpy-driven, representing the improvement in SER photo-stability. Overall, the results highlighted the possibility to use this formulation with improved stability in clinical practice for treatment and prevention of various depressive conditions, such as anxiety disorders.

Keywords: Theoretical chemistry, Pharmaceutical chemistry, Physical chemistry

https://doi.org/10.1016/j.heliyon.2019.e01405

1. Introduction

Serotonin or 5-hydroxytryptamine is an active molecule primarily found in various tissues, including the gastrointestinal tract and central nervous system (CNS) of animals as well as humans [1]. This compound is considered to be one of the most important neurotransmitters in the brain mediating the neuronal activity [2] in various cognitive and behavioral conditions, such as asleep, mood, pain, depression [3], addiction, locomotion, sexual activity, anxiety [4] aggression, and learning [1, 2, 3]. All these functions of SER as a regulatory molecule to maintain homeostasis of the CNS have drawn a lot of attention from the scientific community [5]. In particular, the SER deficiency is associated with the risk of dementia, Alzheimer's disease [6] and various mental disorders, such as schizophrenia, migraine [7, 8], suicidal behavior, infantile autism, eating disorders, obsessive-compulsive disorder [8, 9, 10], and insomnia [11].

Cyclodextrins (CDs) are cyclic oligosaccharides formed by the D-glucopyranoside units via α-(1→4) glycosidic bonds, forming a truncated cone structure. The most common (commercially available) CDs are α-, β- and γ-CDs, consisting of 6, 7, and 8 glucopyranoside units [12, 13]. Due to low cost in CD production, suitable cavity size, effective drug complexation and loading, and high biocompatibility, α-, and β-CDs were found to be the most favorable candidates for biomedical and industrial applications [14, 15]. Additionally, both the complexation and chemical behavior of α-CD, and β-CD is usually similar but the γ-CD is behaving slightly differently, due to the larger mobility of the glucopyranoside moiety. Inside these natural CDs, several derivatives of CDs have also been synthesized. These synthesis CDs are more hydrophilic or hydrophobic than natural CDs. The solubility and stability (light, oxygen and moisture) of guests and drug compounds could be even more improved due to complexation with these chemically modified CDs. All CDs contain a more hydrophilic exterior and a less hydrophobic, less-polar cavity (the dielectric constant of the cavity is close to the 40% ethanol/water mixture) that makes them appropriate for the formation of various inclusion complexes (IC) with drug-like molecules by suitable size. This complexation mechanism is mainly mediated by the hydrophobic interactions between the host (CD) and its guest as the enthalpy-driven release of water molecules (desolvation effect) from the CD cavity. Of course, complexation does not mean that water molecules are completely released from the inside of the cavity and may remain some of the water molecules in the inner cavity [16, 17, 18].

In the pharmaceutical industry, CD-based excipients are applied as drug delivery vectors to improve solubility, stability, pharmacokinetics, and storage conditions of active pharmaceutical ingredients [19]. As serotonin hydrochloride (SER) are sensible into the environmental conditions such as light, oxidation, and heat, it should be protected against undesirable changes during storage or processing by its

https://doi.org/10.1016/j.heliyon.2019.e01405

encapsulation with β-CD. As similarly reported on the formation of β-CD: SER IC, Bisby *et al.* (2007) have investigated the encapsulation of SER into the cavity of β-CD, using both steady-state and time-resolved fluorescence methods where the estimated binding constant at 25 $^{\circ}$C (K_a) were 53.2 and 59.4 M^{-1}, respectively [20]. In the other similar study, Chaudhuri et al. (2010), have studied the encapsulation of SER into the nano-cavities of β-CD by measuring the intrinsic serotonin fluorescence and obtained the value of 126.06 M^{-1} for the associative binding constant of IC [1]. Furthermore, they have done the molecular docking and the semi-empirical calculation and evaluated the molecular interactions among the formation of the IC. The molecular docking observed that the insertion of SER into the cavity of β-CD was implemented with the aliphatic amine side chain closer to the narrower side of the β-CD cavity. And also, the stoichiometry 1: 1 of the host: guest (β-CD and SER) was determined by the semi-empirical calculation [1]. These experiments were also followed by the study of Abbaspour et al. (2011), where the authors analyzed the simultaneous quantification of SER and dopamine using electrochemical sensors [21]. Despite these studies, there is not any comprehensive report on the thermodynamic nature of the process, the detailed characterization of the IC, the effect of this encapsulation on the photo-stability of SER and also the molecular dynamic simulation of the whole process.

In this work, an inclusive study was done on the preparation, characterization, phase solubility, photo-stability, thermodynamics and molecular dynamics of β-CD: SER IC, in order to determine the chemical, physical and molecular properties of this IC. This study could be helpful for the evaluation of the feasibility to use this formulation with improved stability in clinical practice for treatment and prevention of various depressive conditions.

2. Materials and methods

2.1. Materials

The β-CD (98 % purity) with 14% water content, and SER hydrochloride (>98 % purity) have been purchased from the Sigma-Aldrich company (Dorset, UK). The high-purity D_2O solvent was attained from the Merck Company (Darmstadt, Germany). Milli-Q water (UPW) was used for the preparation of phosphate buffered (PBS, 10mM, pH 7.4).

2.2. Complex preparation

2.2.1. Physical mixture method

The (1: 1) molar ratio quantities of the β-CD and SER were weighted accurately and mixed together thoroughly in a mortar.

https://doi.org/10.1016/j.heliyon.2019.e01405

2.2.2. Freeze-drying method

β-CD and SER (1:1 molar ratio) were dissolved in deionized water that deoxygenized by blowing of N_2 gas for 10 minutes and stirred in neutral pH for 24 hours to reach the thermodynamic equilibrium at room temperature. In order to achieve the complete complexation, 200 mg of β-CD and 37.48 mg of SER, were dissolved in 10 mL of the above-mentioned water. Whereas the amount of SER is not in excess respect to the amount of β-CD, there is a little difference between the intended and the realized complex composition, however, the results are poorly affected by the difference. Afterward, the mixture was centrifuged at 10000 rpm for 5 min, for separation pure SER and β-CD from the supernatant, to produce the pallet, which was freeze-dried (VaCo5, Zirbus, Germany), subsequently, at -50 °C and 130×10^{-3} mBar. The powder was stored at -4 °C.

2.3. Phase solubility study

Phase solubility study of β-CD: SER IC was done using the Higuchi-Connors method [22]. In particular, the multiple concentrations of β-CD (0, 0.72, 1.108, 1.43, 1.79, 2.15, 2.51, 2.87 and 3.58 mM) were prepared and dissolved in deoxygenized PBS (10 mM, pH 7.4). After that, 500 μL of SER (5 mg/mL) dissolved in PBS was added to 2500 μL of β-CD. The final mixture was sealed and wrapped in aluminum foil to avoid any changes caused by evaporation, oxidation, and photochemical degradation effects. To achieve the complexation equilibrium, the mixture was placed in the cooling and shaking incubator (Jal Tajhiz, JTSDL40, and IRAN) for 72 hours at 10, 12, 15 and 18 °C. The SER does not oxidize during the inclusion complex formation at ambient temperature. Actually, the rate of oxidation is strongly depended on temperature and increases with increasing temperature. The oxidation process that accompanies with the color change of the SER solution, has been examined at various temperatures and the temperature range was selected on the basis of this factor. Afterward, the samples were filtered through a 0.45 μm Millipore membrane filter, and the SER concentration in the supernatant was measured spectrophotometrically at 276 nm using the UV-vis spectrophotometer (Perkin Elmer, Lambda 265, USA) [19, 23]. The apparent stability constant (K_c) of the complex was calculated from the phase solubility diagrams according to the following Eq. (1):

$$K_c = \frac{slope}{S_0(1 - slope)} \tag{1}$$

Where S_o is the intrinsic SER solubility in aqueous solution in the absence of β-CD.

All spectroscopic analyses were carried out at 10, 12, 15 and 18 °C. The estimated binding constants were used for calculation of ΔG°' using the Gibbs equation, ΔG°' = -RTlnK_c where ΔG°' is the Gibbs free energy of binding (kJ. mol^{-1}). The other

https://doi.org/10.1016/j.heliyon.2019.e01405

thermodynamic parameters ($\Delta H^{\circ\prime}$ and $\Delta S^{\circ\prime}$) were estimated using the following Eq. (2):

$$\ln(K_c) = -\frac{\Delta H^{0\prime}}{RT} + \frac{\Delta S^{0\prime}}{R} \quad (2)$$

Where $\Delta H^{\circ\prime}$, $\Delta S^{\circ\prime}$, R, and T are the enthalpy and entropy change ($kJ \cdot mol^{-1}$), gas constant ($J \cdot mol^{-1} \cdot K^{-1}$) and absolute temperature (K), in that order.

2.4. Complex characterization

The Fourier-transform infrared spectroscopy (FT-IR) spectra of pure SER, β-CD, and β-CD: SER IC were recorded at room temperature in the range of 4000−400 cm^{-1} with a resolution of 4 cm^{-1} by the FT-IR spectrometer (JASCO, FT/IR-6300, and Japan). The samples were prepared on a KBr pellet in vacuum desiccators under a pressure of 0.01 torr. Proton nuclear magnetic resonance spectroscopy (^{1}H-NMR) for SER, β-CD, and IC was carried out in D_2O at 25 °C in the range of 0−10 ppm by the ^{1}H-NMR spectrometer (Bruker, Ultra shield 400 MHz, Germany). The observed sharp signal around 4.7 is related to HDO that produced due to the exchange of protons between D_2O and β-CD. The HDO resonance, as the lock frequency, set to 4.69 ppm in order to get uniform values for the chemical shifts [24].

The chemical shift change (Δδ) was calculated according to the Eq. (3):

$$\Delta\delta = \delta_{complex} - \delta_{free} \quad (3)$$

Where $\delta_{complex}$ and δ_{free} are the chemical shifts of IC and free β-CD or free SER, respectively. The microstructure of β-CD, SER, and their IC was analyzed using the field-emission scanning electron microscope (FESEM) (Zeiss, Sigma, VP-500 EDS, Germany) at the acceleration voltage of 15 kV. The samples were coated in a vacuum with a layer of gold. The X-ray powder diffraction (XRD) using the X-ray diffractometer (D8 ADVANCE, Bruker, Germany) was applied to investigate the crystalline or amorphous composition of the analyzed substances. The XRD patterns of β-CD, SER, and β-CD: SER IC were measured using the copper anode tube with a nickel filter, Kα radiation wavelength of 1.5406 Å, voltage of 40 kV, current density of 50 mA and diffraction angle (2θ) in the range of 5−80° at the rate of 0.05°/min. The samples were packed tightly in a rectangular aluminum container to be exposed to the beam. The thermogravimetric analysis (TGA), differential thermogravimetric (DTG), and differential thermal analysis (DTA) curves of β-CD, SER, and β-CD: SER IC were produced by using the TGA 2050 thermogravimetric analyzer (TA-2050, Machinio, USA). In particular, 2−3 mg of each substance were analyzed under heat conditions from 25 to 900 °C and N_2 atmosphere flow (25 $mL \cdot min^{-1}$) with the heating rate of 10 °C/min. The induced circular dichroism (ICD) spectra of β-CD, SER, and β-CD: SER IC (0.5 mg/mL) were obtained in

https://doi.org/10.1016/j.heliyon.2019.e01405

PBS (10 mM, pH 7.4) by the CD spectrometer (Aviv, Model-215, USA). The near-UV region was scanned between 250 to 350 nm at room temperature.

2.5. Loading capacity and encapsulation efficiency analyses

200 mg of β-CD and 37.48 mg of SER were dissolved in 10 mL of deionized, deoxygenated water. Afterward, the mixture was centrifuged at 10000 rpm for 5 min to produce the pallet, which was freeze-dried (VaCo5, Zirbus, Germany), subsequently, at -50 °C and 130×10^{-3} mBar. A 1 mg/mL solution of the obtained powder (IC) was prepared in deoxygenized water and then equilibrated by stirring for overnight at ambient temperature. The amount of SER entrapped in the β-CD: SER IC (SER_{exp}) was determined spectrophotometrically by measuring the absorbance at 276 nm. The molar extinction coefficient (ε) of SER was taken the average value of ε for free and bound SER. All measurements were done in triplicate [25]. The encapsulation efficiency, EE, and the loading capacity, LC, of solid β-CD: SER IC were determined according to the following equations:

$$LC(\%) = \frac{SER_{\exp}(mg)}{Inclusion\ complex(mg)} \tag{4}$$

$$EE\% = \frac{SER_{\exp}(mg)}{SER_T(mg)} \times 100 \tag{5}$$

Where SER_T is the complexed (trapped) and initial (total) amounts of SER, respectively.

2.6. Photo-stability analysis

The photo-stability analysis of free and complexed forms of SER in the aqueous solution and solid state was performed using natural light from the sun. For the liquid and solid states, 100 μM of the SER and β-CD: SER IC aqueous solution (1 mg/mL) and 10 mg of the same substances as powder were prepared to be exposed to the sunlight for 8 (aqueous solution) and 3 (solid) days. During the decomposition of SER, a hypochromicity in UV spectrum of SER was observed while no new peak detected. It has been examined that the absorption at 276 nm totally vanished at infinite time, hence, the absorbance at this wavelength could be proportional to the amount of undecomposed SER. According to the recorded UV-vis spectra of IC and pure SER, in the range of 240−480 nm, the time monitoring at 276 nm (λ_{max}) would provide the necessary data for evaluation of photo-stability.

2.7. Computational methods

The structure of β-CD was downloaded from the R.E.DD.B project website [26] The protonated form of SER structure was built by the GaussView 5.0 program [27] and

https://doi.org/10.1016/j.heliyon.2019.e01405

minimized and optimized by the Gaussian 09 software [28] with the B3LYP method and 6-311++G (d, p) basis set. The rigid-flexible molecular docking was executed using the AutoDock 4.2.6 program [29] with the grid box set to 40 × 40 × 40 points and grid spacing of 0.375 Å in each dimension. The Lamarckian genetic algorithm was applied using default values. For molecular dynamics (MD) simulations, the AMBER 12 (Assisted Model Building with Energy Refinement) software [26, 30] was chosen with the q4md-CD force field as a combination of the GLYCAM04 and Amber99SB force fields to generate the correct CD topology. The GAFF force field [31] was implemented to produce the topology for SER with the restrained electrostatic potential (RESP) charges via the calculation of the SER partial charges. Accordingly, we have used the charge method implemented in GAFF as HF/6-311++G** RESP charge. In fact, the Antechamber module has been used to assign the net charges from the Amber parameter database, which has been generated by the Gaussian 09 software [32, 33].

The analyzed structures were solvated in a 10 Å truncated octahedron box consisted of the TIP3P (three-point transferable intermolecular potential 3P) water molecules [34]. The MD simulations were performed according to the standard MD protocol available in the literature elsewhere [17, 33]. Initially, the systems were equilibrated by performing the energy minimization of the system by the steepest descent algorithm for at least 10000 steps. Next, the system was heated gradually from 0K to 300K as the equilibration run (NVT) to keep the system's volume and temperature constant in 1 atm and 300 K, respectively. The isotropic position scaling and the method of Berendsen thermostat has been used, respectively. The Particle-Mesh Ewald (PME) method was applied to maintain the long-range electrostatic interactions. A 10 Å cutoff was used for both van der Waals interactions and PME. To monitor the system's equilibrium convergence, the density, temperature and energy parameters were examined. Finally, a 50 ns MD production run with constant pressure and temperature (NPT), was carried out combined with the generalized Born (MM-GBSA) or the Poisson-Boltzmann (MM-PBSA) surface area explicit solvation models [29, 30, 35, 36].

3. Result and discussions

3.1. Phase solubility isotherms and thermodynamics of complex formation

The phase solubility isotherms were measured to assess the effect of β-CD for the improvement of SER solubility, determining the complex stoichiometry and apparent stability constant (K_c) value. As shown in Fig. 1a, the SER solubility has shown the linear increase of SER concentration at 10, 12, 15 and 18 °C, belonging to the A_L-type group and indicating the 1:1 mole ratio between SER and β-CD in IC.

https://doi.org/10.1016/j.heliyon.2019.e01405

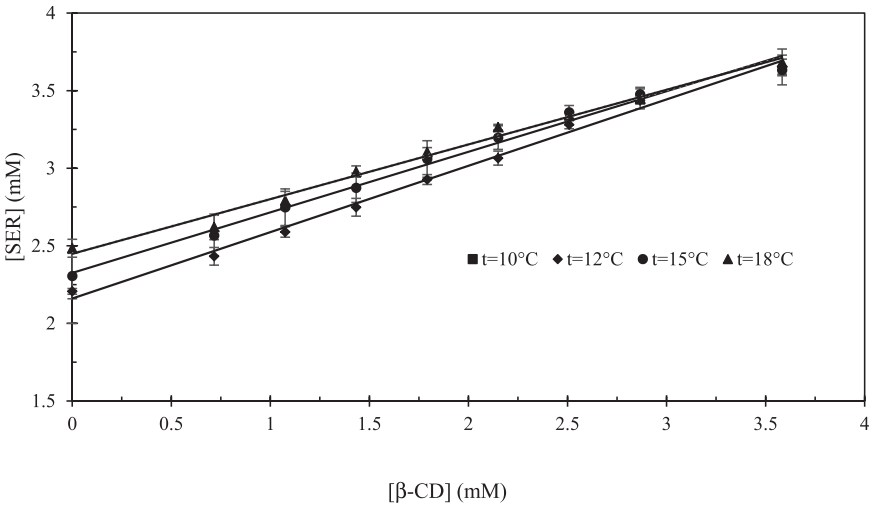

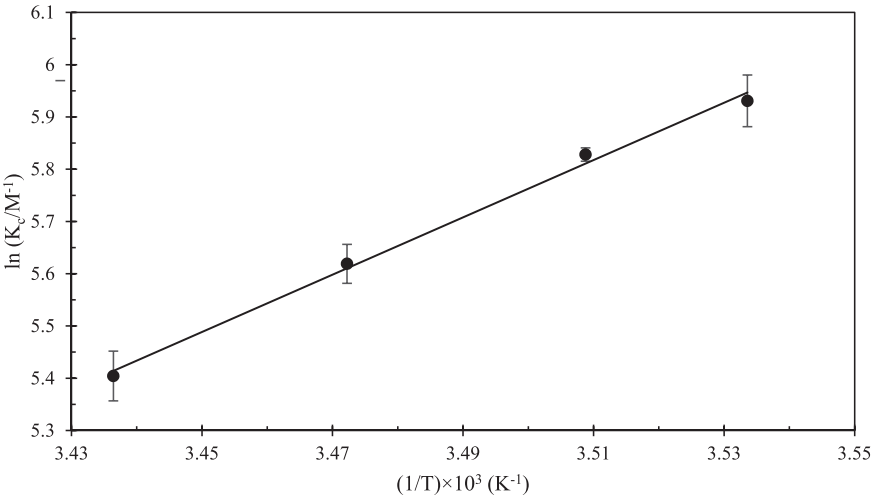

Fig. 1. The phase solubility diagram in PBS (10 mM pH 7.4) and at various temperatures. b) The van't Hoff plot for the formation of β-CD: SER IC ($R^2 = 0.996$).

The SER solubility (S_0) in the presence of β-CD was observed to be elevated in parallel with the elevating temperature. The K_c values were and itemized in Table 1 according to the van't Hoff equation (Eq.2). It is clear from Fig. 1b and Table 1, that the K_c values were observed as the exothermic chemical reaction ($\Delta H\underline{o}' < 0$) of β-CD: SER IC. On the other hand, the main driving force for complex formation was considered to be the release of enthalpy-rich water from the CD cavity [12]. Thus, the complex formation was mainly driven by the hydrophobic interactions due to the water displacement from the β-CD binding site, establishing van der Waals interactions, and H-bond formations between the host and the guest. Moreover, the negative $\Delta S\underline{o}'$ parameter indicated the increase in the system's order in the complex formation, reducing the translational and rotational degrees of freedom [37].

https://doi.org/10.1016/j.heliyon.2019.e01405

Table 1. Phase solubility constants (K_c) and the estimated thermodynamic quantities for the formation of β-CD: SER IC at various temperatures.

T(K)	S_0 (M)	*Slope*	R^2	K_c (M^{-1})	$\Delta G^{\circ\prime}$ (kJ/mol)	$\Delta H^{\circ\prime}$ (kJ/mol)	$\Delta S^{\circ\prime}$ (kJ/mol)
283 ± 0.10	(2.074 ± 0.080)×10^{-3}	0.438 ± 0.016	0.990	376.446 ± 37.468	-13.955 ± 0.470	-45. 595 ± 9.268	-111.802 ± 31.088
285 ± 0.10	(2.160 ± 0.134)×10^{-3}	0.423 ± 0.012	0.994	339.672 ± 16.895	-13.810 ± 0.236	-45. 595 ± 9.268	-111.526 ± 31.692
288 ± 0.10	(2.325 ± 0.409)×10^{-3}	0.391 ± 0.007	0.989	275.601 ± 10.420	-13.455 ± 0.181	-45. 595 ± 9.268	-111.598 ± 31.551
291 ± 0.10	(2.449 ± 0.279)×10^{-3}	0.352 ± 0.007	0.988	222.341 ± 8.727	-13.075 ± 0.190	-45. 595 ± 9.268	-111.751 ± 31.195

In comparison with the previous works, the obtained K_c value at 25 °C (134.83 M^{-1}) is close to the reported value by Chaudhuri et al. (2010) (126.06 M^{-1}), while is about two times greater than the reported values by Bisby *et al.* (2007) (53.2 and 59.4 M^{-1}). This could be related to the different using methods for estimation of associative equilibrium constant and different incubation times for achievement of equilibrium. This time in our work was 72 hours while it was 1 hour and a few minutes in the work of Chaudhuri et al. and Bisby et al. (2007), respectively. It looks the achievement of equilibrium is suspicious in the previous works. The thermodynamic nature of IC, on the basis of enthalpy and entropy changes, that could provide the valuable information about the molecular nature of the interactions, has not been evaluated in the previous works, hence, our work is the first report in this regard.

3.2. Complex chemical characterization

3.2.1. Fourier-transform infrared spectroscopy

FT-IR is a useful method, characterizing and comparing CD structures complexed with different drugs as ICs on one hand and uncomplexed molecules on the other. The FT-IR spectra of β-CD, SER, and β-CD: SER IC are displayed in Fig. 2, where β-CD (Fig. 2a) exhibited a prominent absorption band at 3391 cm^{-1} for the O-H stretching vibrations, 1157 cm^{-1} for the C-O stretching vibrations in hydroxyl groups, and 2928 cm^{-1} for the C-H stretching vibrations. Additionally, the peaks at 1029 cm^{-1} for the O-C-O ether linkage stretching vibrations and at 1418 cm^{-1} for the O-H bending vibrations were also detected [38]. The FT-IR spectrum (Fig. 2b) of SER showed an absorption band at 3425 cm^{-1} for the phenolic O-H stretching vibrations, 3421 and 1199 cm^{-1} for the -NH_3^+ stretching vibrations, but with less intensity, 3394 and 1305 cm^{-1} for the aromatic N-H stretching and the C-N stretching vibrations, 3034 and 2939 cm^{-1} for the C-H stretching vibrations, 1455, 1367 cm^{-1} for the C-H bending vibrations, and 1582 and 1305 cm^{-1} for the C=C and C-C stretching vibrations. The values near 1000 cm^{-1} threshold were related to the breathing mode of the substituted phenyl ring [38]. The β-CD and β-CD: SER IC spectra (Fig. 2d) exhibited the transmission of the hydrogen-bonded region (3000-3500 cm^{-1}) that its intensity for IC is lower than free β-CD. The

https://doi.org/10.1016/j.heliyon.2019.e01405

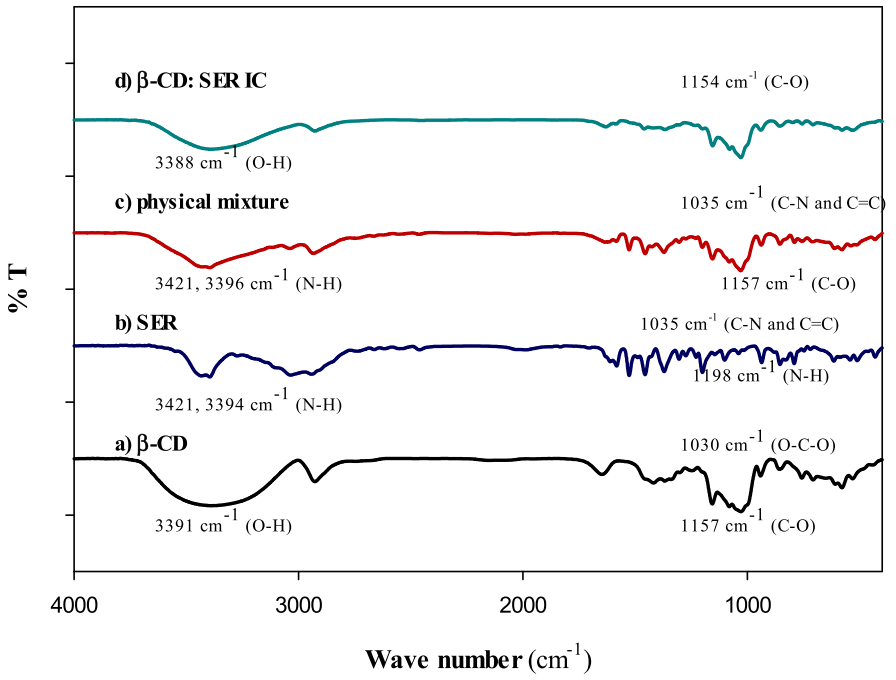

Fig. 2. FTIR for a) β-CD, b) SER, c) physical mixture (β-CD: SER) and d) β-CD: SER IC.

decrease in the peak intensity could be related to the replacement of SER with water molecules into the cavity of β-CD. The IC spectrum also contains the absorption bands at 1154 cm^{-1} corresponding to the C-O stretching vibrations and 1418 cm^{-1} for the bending vibrations with a blue shift but with less intensity than in the spectrum observed for the pure β-CD form. The spectrum at 1030 cm^{-1} displayed a sharp decline in comparison to β-CD for the O-C-O stretching vibrations. The spectra at 1199 and 1304 cm^{-1} for the aliphatic and aromatic C-N vibrations represented a few shifts for SER and some shifts with considerably different intensity for IC. The peaks before 1000 cm^{-1} threshold for SER spectrum belonged to the aromatic group with the decreased intensity compared to the same molecule in IC. This phenomenon could be due to the insertion of SER molecule into the less hydrophobic cavity of β-CD, which triggered the spectral changes (i.e. significant frequency shifts, broadening and/or changes in shape) in the formation of β-CD: SER IC, representative the role of van der Waals forces and H-bonding in the complexation. The FT-IR spectrum of the physical mixture (SER and β-CD) was also recorded and compared with the spectrum of the IC for removing of any ambiguity according to the presented interpretation. As shown in Fig. 2, the spectrum of the physical mixture has several differences with the spectrum of IC, representing the bond formation between SER and β-CD in the IC.

https://doi.org/10.1016/j.heliyon.2019.e01405

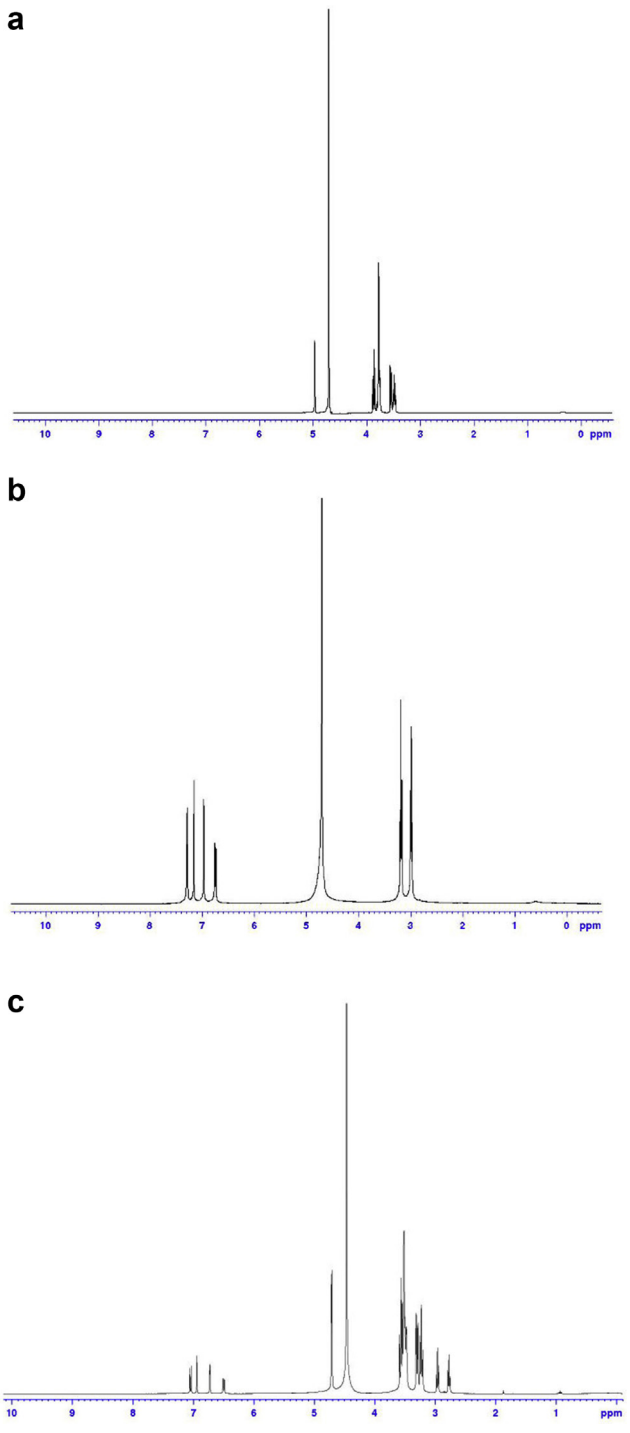

Fig. 3. ^{1}H-NMR belonging a) β-CD, b) SER and c) β-CD: SER IC in D_2O.

https://doi.org/10.1016/j.heliyon.2019.e01405

3.2.2. ^{1}H-NMR spectroscopy

The IC structure was also monitored by ^{1}H-NMR spectroscopy [39]. The ^{1}H-NMR spectra generate an obvious difference between IC and free guest and host. In β-CD, H-3 and H-5 protons situate in the cavity of the β-CD. H-3 protons occur in the wide side of the cavity and H-5 protons belong to on the narrow side of the cavity, thus these two protons have been influenced by the complexation and show a chemical shift. As shown in Fig. 3c, for studying the inclusion behavior of β-CD: SER IC, the ^{1}H-NMR spectra of β-CD (Fig. 3a), SER (Fig. 3b) and β-CD: SER IC (1:1) were compared. Fig. 3a and b show a number of spectrum at 3.85 ppm for H-3 and 3.75 ppm for H-5 of free β-CD and 7.26 ppm for H-5 of free SER, whereas ^{1}H-NMR spectrum of the IC (Fig. 3c) contains the following peaks: 3.63 ppm for H-3 ($\Delta\delta$ = -0.22 ppm), 3.52 ppm for H-5 ($\Delta\delta$ = -0.23 ppm) and 7.05 ppm for H-5 ($\Delta\delta$ = -0.21 ppm). All of the results corresponding to the chemical shift change presented in Table 2. The most chemical shift change is observed for H-5 in β-CD and H-5 in SER which could be an indication that SER is more located on the narrow side of the β-CD cavity. Consequently, the ^{1}H-NMR study confirms the formation of IC and specifies the location of SER in the narrow side of the β-CD cavity.

3.2.3. Field emission scanning electron microscopy

The FE-SEM approach is also a useful approach to explore the IC structure. The SEM micrographs of SER, β-CD, and β-CD: SER IC are displayed in Fig. 4. The

Table 2. ^{1}H-chemical shift (δ [ppm]) belonging to pure β-CD, SER and β-CD: SER IC in D_2O.

β-CD	$\delta_{\beta\text{-CD}}$ (ppm)	$\delta_{complex}$ (ppm)	Δδ (ppm)
H-1	4.94	4.74	-0.20
H-2	3.52	3.48	-0.04
H-3	3.85	3.63	-0.22
H-4	3.47	3.46	-0.01
H-5	3.75	3.52	-0.23
H-6	3.76	3.58	-0.18
SER	δ_{SER} (ppm)	$\delta_{complex}$ (ppm)	Δδ (ppm)
H-5	7.26	7.05	-0.21
H-3	6.78	6.93	0.15
H-6	6.74	6.72	-0.02
H-8-1,8-2	3.17	3.22	0.05
H-9-1,9-2	2.97	2.95	-0.02
H-7	7.14	7.02	-0.12

https://doi.org/10.1016/j.heliyon.2019.e01405

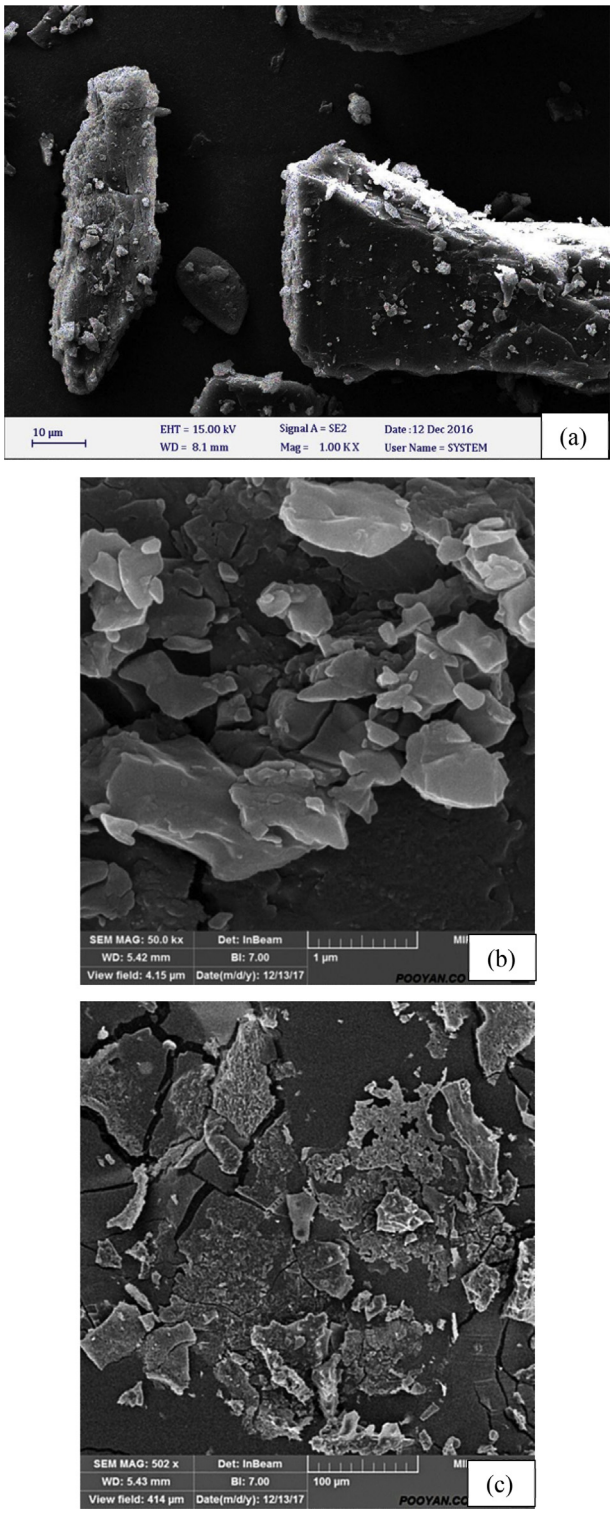

Fig. 4. FE-SEM micrograms for a) β-CD, b) SER and c) β-CD: SER IC.

https://doi.org/10.1016/j.heliyon.2019.e01405

pure β-CD form was found as crystal nano-cavity parallelogram in shape (Fig. 4a). On the other hand, SER was rearranged as plate-shaped crystals (Fig. 4b). However, β-CD: SER IC appeared to be as a compact amorphous powder without any apparent crystallization (Fig. 4c). Overall, all the SEM differences for IC indicated and confirmed the formation of β-CD: SER IC.

3.2.4. X-ray powder diffraction

The XRD method is a valuable technique for the determination of crystallinity of the analyzed substances in powder form. As the CD complexation accompanies the disappearance of some characteristic peaks and the appearance of some novel ones, this all might be a compelling evidence of the complex formation [40]. The XRD patterns for SER, β-CD, and β-CD: SER IC, and physical mixture of SER and β-CD, are displayed in Fig. 5. Especially the β-CD and SER patterns displayed the numerous sharp peaks characteristic of their crystallinity. In particular, the XRD pattern (Fig. 5a, b) showed several high-intensity peaks at various diffraction angles (2θ) of 10.34, 14.70, 22.75 and 40.65° for β-CD and 11.25, 15.75, 22.55, 24.55 and 26.85° for SER, suggesting the crystal structure of both molecules. On the contrary, the XRD diffractogram of β-CD: SER IC (Fig. 5d) was discovered to be in amorphous form with the crown pattern, without any peaks at 14.70 and 24.55° and with two peaks at 10.85 and 12.55°. This XRD pattern showed less intense and highly diffused peaks of SER which indicated to a reduced ordering of crystal lattice, demonstrating the formation of the amorphous solid state. In this prepared IC, there was a reduction in crystallinity of the SER as compared to a pure sample which reflects that the SER is dispersed in the β-CD. Moreover, the comparison of the XRD patterns of the physical mixture (Fig. 5c) and IC (Fig. 5d), could be represented the bond formation between SER and β-CD in the IC.

3.2.5. Thermal analysis

The thermal stability of β-CD, SER and IC were measured by the TGA method and its modifications (DTG and DTA). As shown in Fig. 6a and b (dash line), the stability curves of the pure β-CD form displayed initially a small mass loss of 10% at about 46 °C, which can be ascribed to the loss of water associated with β-CD. The second weight loss, in the range of 276−362 °C with a 75 % mass loss was due to the degradation of this molecule. The pure SER (dot line) compound started to decompose at about 231 °C with 33% mass loss followed by degradation until 478 °C with 31% mass loss (Fig. 6a and b). In the TGA (Fig. 6a) and DTG curves (Fig. 6b) of β-CD: SER IC (line) indicated a first mass loss at low temperature (around 39 °C, ~3 %) that could be associated with the replacement of some water molecules by SER, while the degradation of IC was detected in the range of 200−353 °C with a 41 % mass loss. This degradation temperature shift is indicative of the SER

https://doi.org/10.1016/j.heliyon.2019.e01405

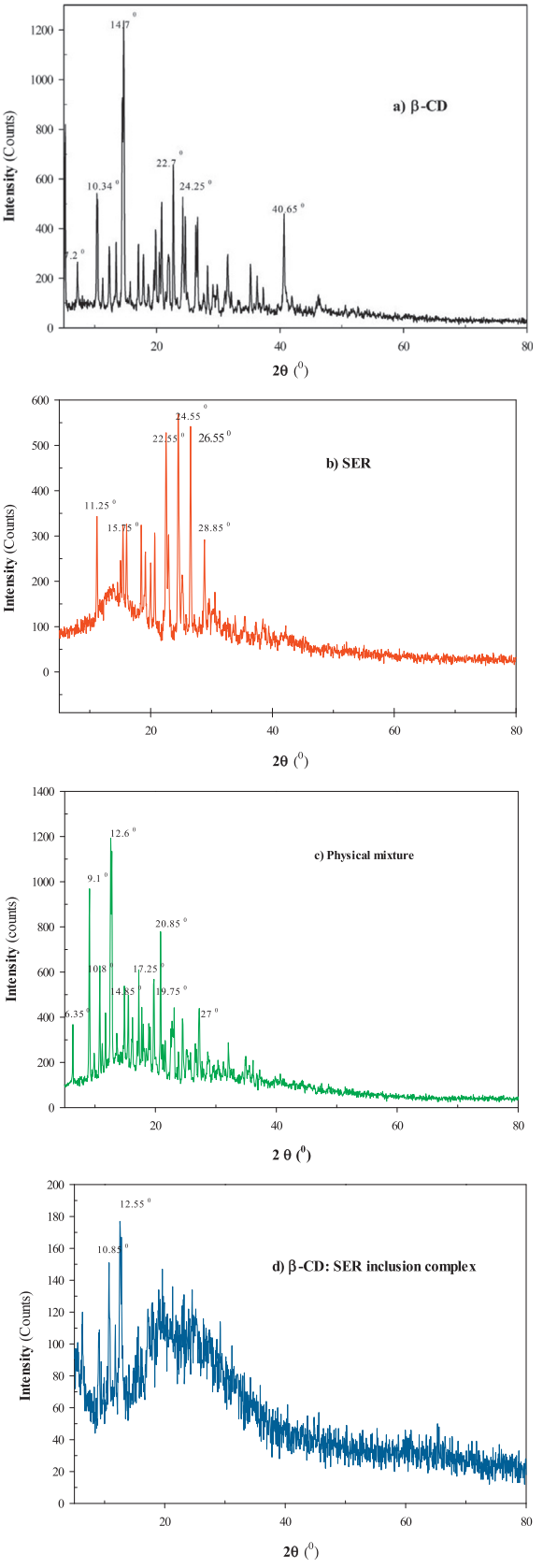

Fig. 5. XRD for a) β-CD, b) SER, c) physical mixture (β-CD: SER) and d) β-CD: SER IC.

https://doi.org/10.1016/j.heliyon.2019.e01405

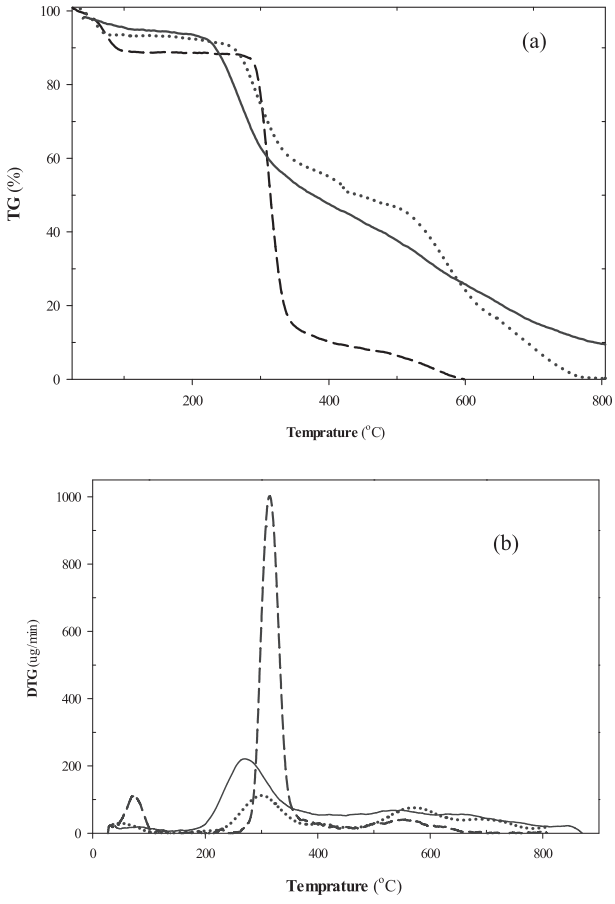

Fig. 6. The TGA (a) and DTG (b) curves for β-CD (dash line, - - -), SER (dot line, …..) and β-CD: SER IC (line, —).

incorporation into the β-CD cavity and represents the improvement of the complex thermal stability. Additionally, the DTA studies also confirmed the encapsulation and protection of SER within the β-CD binding site. The DTA curve of the pure β-CD form (Fig. S1, dash line) revealed one exothermic at 547 °C and two endothermic peaks at 82 and 311 °C. Similarly, the DTA curve of the pure SER substance (Fig. S1, dot line) depicted also one exothermic peak at 303 °C and two endothermic peaks at 67 and 169 °C, while the complexed SER compound contains only one endothermic peak at ~257 °C and one exothermic peak at 541 °C (Fig. S1, line), suggesting the formation of β-CD: SER IC in the solid state.

3.2.6. Induced circular dichroism spectroscopy

The ICD spectroscopy is a helpful method to study the IC structure between the β-CD and optically active molecules [41]. The insertion of a guest molecule to the cavity of β-CD is usually accompanied by the optically active environment observed as the ICD peak. According to the theoretical Harata's rule, this peak is positive if the

https://doi.org/10.1016/j.heliyon.2019.e01405

transition dipole moment of gust molecule aligns parallel or at some angle to the β-CD molecular axis or it is negative in the case of negative in perpendicular alignment [35]. For Fig. 7 it is clear that the ICD spectrum of SER, β-CD, and β-CD-SER IC appears to be positive ICD at 286 nm with $\Delta\varepsilon = 3.07\ cm^{-1}.M^{-1}$ demonstrating the insertion of SER into the β-CD cavity.

3.3. Loading capacity and encapsulation efficiency

The amount of SER in the freeze-dried β-CD: SER IC was evaluated spectrophotometrically at 276 nm. According to Eqs. (4) and (5), the values of (5.92 ± 2.34) % and (31.61 ± 1.25) % were obtained for the LC % ((mg of encapsulated SER/mg of complex powder) ×100) and encapsulation efficiency (EE %), respectively. These results represent the suitability and high capacity of β-CD for encapsulation of SER. Moreover, these values are in agreement with the formation of 1:1 complex, found out from the phase solubility studies.

3.4. Photo-stability

Because of the presence of phenolic hydroxyl and amine groups, SER can give hydrogen atoms to radicals, thus acting as radical chain terminators and is unstable in various environmental conditions such as light, oxygen, and moisture. Therefore, its protection from these damaging agents is proposed. The engagement of SER in the cavity of β-CD could be improved its stability against these factors, especially UV-vis light. The photo-degradation experiments were designed in order to examine this probable photo-stability improvement of SER. The photo-degradation reaction was followed by a recording of UV-vis spectra of SER and β-CD: SER IC in liquid and solid states at various time.

The UV-vis absorption spectra of SER and β-CD: SER IC in liquid and solid states were indicated in Fig. S2 and Fig. S3, respectively. Fig. S4a, b shows the variation of

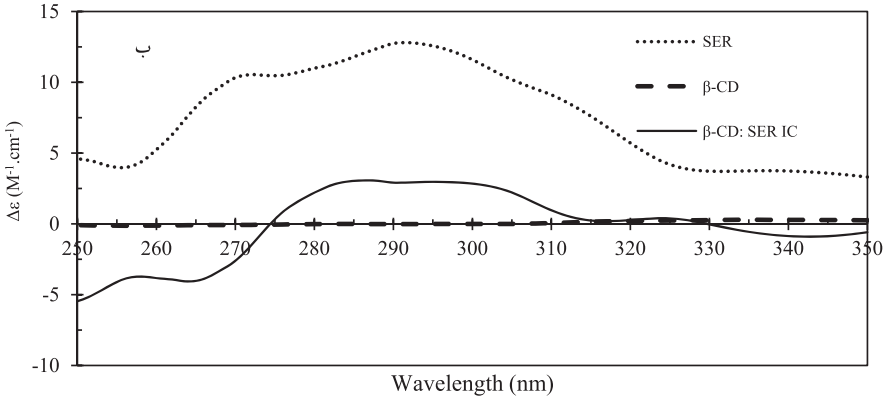

Fig. 7. The ICD spectra of β-CD (dash line, - - -), SER (dot line, …..) and β-CD: SER IC (line, —) at 250–350 nm in PBS (10 mM, pH 7.4).

https://doi.org/10.1016/j.heliyon.2019.e01405

A_t/A_0 *vs.* time (hour) for free SER and β-CD: SER IC, where A_0 and A_t are the absorbance at 276 nm at initial and after exposing to sunlight time of t, respectively. Supposing a pseudo-first order reaction for the photo-degradation process, the apparent rate constant (k) can be determined by means of the following equation:

$$\ln\left(\frac{A_t}{A_0}\right) = -kt \tag{6}$$

Where k is the apparent pseudo-first order rate constant.

The estimated k values and half-life time ($t_{0.5}$) for the photo-degradation process of the investigated compounds are reported in Fig. S4c, d and Table 3, where these parameters were significantly improved for the complexed SER form in the liquid state. This situation could be explained that the complexed SER variant in the solid state is more exposed to the sunlight, which is detrimental to the overall stability.

3.5. Computational methods

3.5.1. Molecular docking

The molecular docking experiments predicted the complexation process through the hydrogen bonds formation between β-CD and protonated SER, where the hydroxyl groups of β-CD glucopyranoside units interact with the ammonium functional group of SER. The H-bond formations in the best molecular docking pose are shown in Fig. 8 with the ΔG° value of -5.91 kcal/mol to be in agreement with the experimental ICD and ^{1}H-NMR data.

3.5.2. MD simulation

MD simulations were computed for the precise determination of molecular structure and interaction of the β-CD: SER IC. MD run for the β-CD was performed in a box of water for 50 ns at a pressure 1 atm and temperature 300 K.

Table 3. Pseudo-first order reaction for the photo-degradation process, the apparent rate constant (k) and half-life time ($t_{0.5}$) in a) aqueous solution state and b) solid state.

a) Liquid state	**SER**	**β-CD: SER IC**
k ($\times 10^3$) (hour^{-1})	6.03 ± 0.30	1.60 ± 0.08
$t_{0.5}$ (hour)	114.87 ± 5.74	432.97 ± 21.65
b) Solid state	**SER**	**β-CD: SER IC**
k ($\times 10^3$) (hour^{-1})	29.60 ± 1.50	8.50 ± 0.42
$t_{0.5}$ (hour)	23.41 ± 1.17	81.53 ± 4.08

https://doi.org/10.1016/j.heliyon.2019.e01405

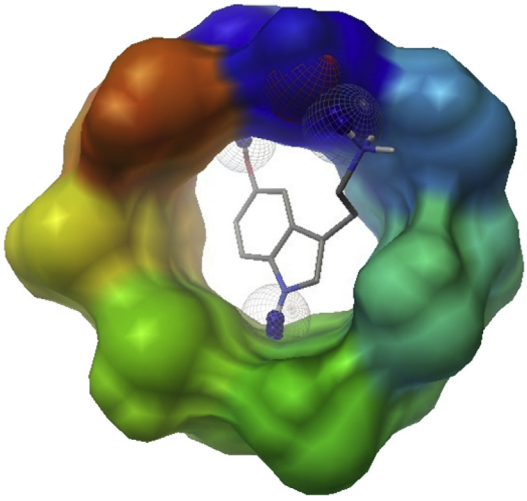

Fig. 8. Molecular docking for β-CD: SER IC.

For analysis, the PTRAJ and CPPTRAJ modules of AMBER 12 program were applied to compute the structural changes, root mean square displacement (RMSD), radial distribution function (RDF), the distance between the center of gravity of SER ring and β-CD and the implicit solvation models in MM-GBSA and MM-PBSA calculations [26, 42].

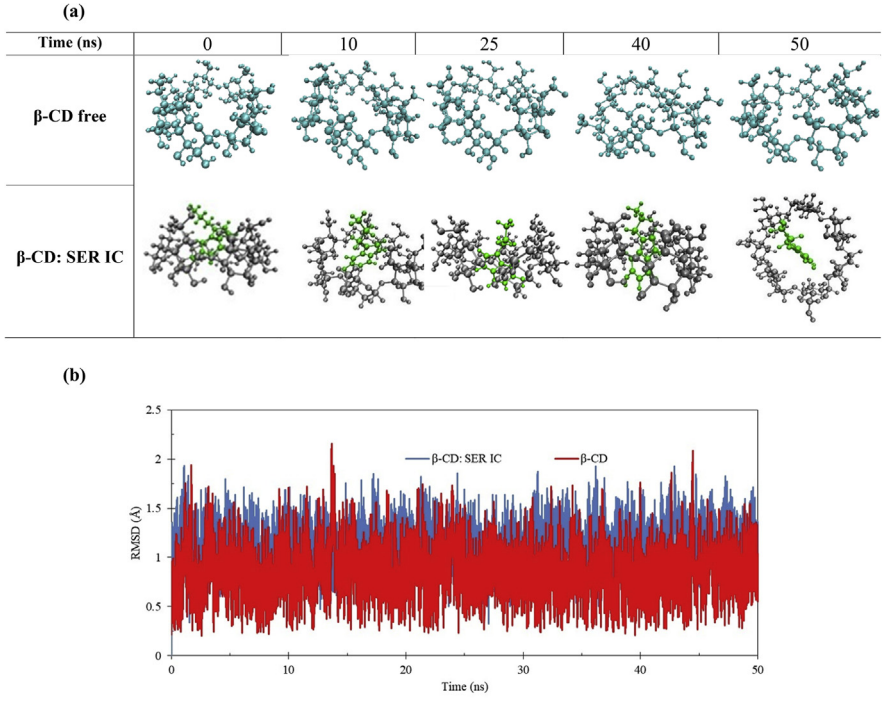

Fig. 9. a) Snapshots of in the free β-CD and β-CD: SER IC in 0, 10, 25, 40 and 50 ns. b) RMSD of free β-CD and β-CD: SER IC during 50 ns simulation time.

https://doi.org/10.1016/j.heliyon.2019.e01405

Fig. 9a displays the structure of β-CD: SER IC in 0, 10, 25, 40 and 50 ns. The snapshots of β-CD and β-CD: SER IC show that SER molecule has finally entered into the cavity of β-CD. These results are in agreement with the ^{1}H-NMR and ICD spectroscopies and molecular docking results. The stability of complexed β-CD and free β-CD was compared by calculation of RMSD of the β-CD relative to those obtained from docking, in free and complex state and then the stability of structure through 50 ns was investigated [43]. In Fig. 9b, the RMSD values of the β-CD in free (red) and IC with SER (blue) states have been shown during the 50 ns of simulation time. The RMSD values in free and complexed β-CD fluctuated about the mean values of 0.8477 ± 0.2467 Å and 1.1122 ± 0.2077 Å, respectively. As can be seen in Fig. 9b, the RMSD values were relatively stable, which indicated the complex had converged and equilibrated state after MD simulation. The comparison of the structural changes (Fig. 9a) and RMSD of free and complexed β-CD (Fig. 9b), could conclude that SER might form a more stable IC with β-CD [44].

The RDF parameter was analyzed by using the CPPTRAJ module. The RDF plots are responsible for valuable data on how water molecules are distributed inside and around the oxygen atoms of glucopyranoside unit of β-CD in free and complex states and hydrogen and oxygen atoms of SER in the IC with the 10 E cutoff [45]. Each D-glucose unit of β-CD has a similar environment when the β-CD is immersed in a bulk aqueous medium (Fig. 10a). This fact arises from the flexibility of the β-CD and the formation of hydrogen bonds between β-CD and the surrounding water molecules. Because of the β-CD relatively flexible in solution, the glucose units should display significant fluctuations. Fig. 11 indicates five RDF curve of free and complexed β-CD in each distribution, with water molecules distributed outside and inside the cavity of the CD and bound to its outer wall, respectively. The first hydration shell of β-CD is formed by these water molecules. These plots describe the pair correlation functions of the oxygen atoms of ordered water molecules

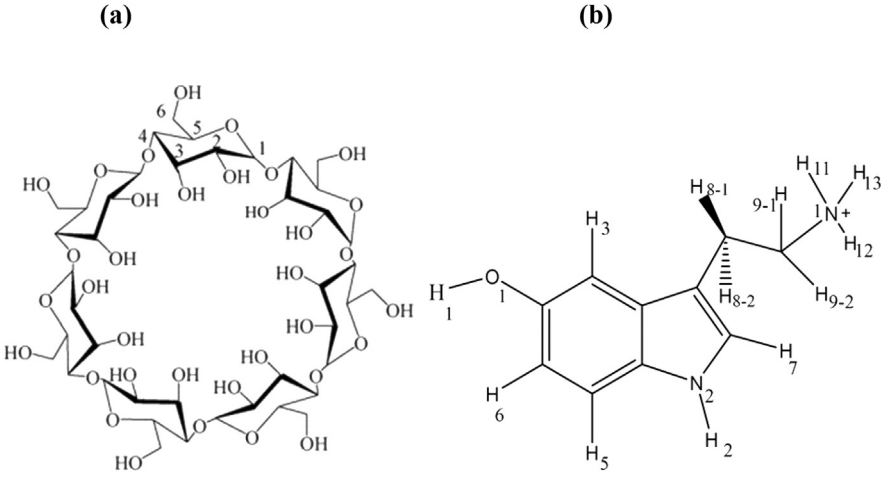

Fig. 10. a) A D-glucose unit in of β-CD (n = 7), b) SER molecule.

https://doi.org/10.1016/j.heliyon.2019.e01405

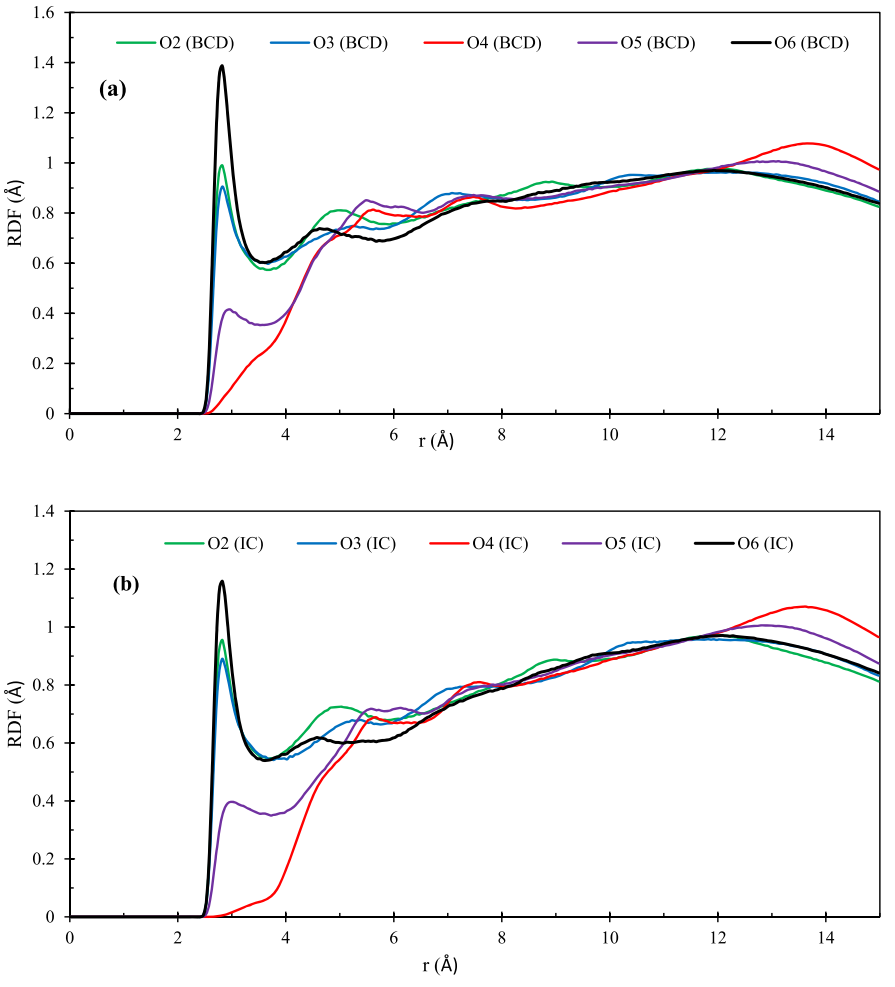

Fig. 11. a) RDF of waters around the oxygen atoms (O2, O3, O4, O5 and O6) for a) free β-CD and b) β-CD: SER IC.

with the O2, O3, O4, O5 and O6 atoms of β-CD. As shown in Fig. 11a and b, the RDF of O2, O3, O5 and O6-free-β-CD and the RDF of O2, O3 and O6-complexed-β-CD are very similar. These peaks are at a range distance of 2.4−3.4 Å, indicative of hydrogen bonding interactions. In this region, the maximum values of the peaks correspond to the water molecules in the exterior cavity of the β-CD (with r ≈2.8 Å, g(r) ≈1.39 approximately) [46]. The complexed β-CD peak has been shown in (Fig. 11b). The intensity of maximum value of the O2, O3 and O6 peaks in complexed state decreases relative to the free β-CD. The O5 has been located inside the cavity and has been bonded with ether group. O5 in free β-CD (r ≈ 3 Å, and g(r) ≈0.42 approximately) has the highest peak intensity (Fig. 11a, while, O5 in complexed β-CD (r ≈3 Å, and g(r) ≈ 0.39 approximately), due to exit the water molecules and insertion the SER molecule, hence it cannot form a hydrogen bond with water molecules and peak maximum is not remarkable and the peak intensity is reduced (Fig. 11b). Since O4-β-CD are in the form of a glycosidic

https://doi.org/10.1016/j.heliyon.2019.e01405

bond and are partially separated by the hydrophobic carbon skeleton, therefore it is not available for water molecules. Consequently, it cannot form any hydrogen bond with water. This result is confirmed by ^{1}H-NMR spectroscopy and the location of SER in the narrow side of the β-CD cavity. As observed Fig. S5a, the RDF of H11, H12, and H13 of SER, are quite similar and range distance r ≈ 2 Å, indicative of the formation of hydrogen bonding interactions with the water molecules, located around the cavity, which are removed from the cavity during the formation of IC of β-CD: SER. The H1-SER (r ≈ 2.1 Å, and g(r) ≈ 0.4 approximately), according to the predicted results of molecular docking, formed the H-bond with O4-β-CD of D-glucose unit, hence it cannot form a hydrogen bond with water molecules and peak maximum is not remarkable. The H2 and N2-SER have been situated inside the less hydrophobic cavity of β-CD, therefore it cannot form a hydrogen bond with water molecules and has not remarkable peak. As observed in Fig. S5b, the RDF between the mass center of complexed β-CD and Ow has been reduced related to the free β-CD and Ow that this may be the removal of water molecules and insertion of SER into the cavity of β-CD.

For understanding the dynamic behavior and the extent of distortion of β-CD before and after complex formation, distance values of O4-O5 calculated in the free and complexed state of β-CD. As illustrated in Fig. S6, the distance values were 1.1986, 1.3323 and 1.2469 ± 0.1123 Å for initial, final and average of distance values for free β-CD, and 1.1191, 1.2241 and 1.2426 ± 0.1070 Å for β-CD: SER IC, respectively. As shown in β-CD and β-CD: SER IC snapshots, these values do not show changes in distance and do not change the conformation of β-CD during the formation of IC. Also, the distance from the center of gravity of β-CD to the center of gravity of SER was determined during 50 ns of simulation time. Fig. 12, showed the distance plots of the center of mass of the O4-β-CD: SER during the 50 ns of simulation. The estimated initial, final and average distance values were 1.8518, 0.5697 and 1.4360 ± 0.7676 Å, respectively. After the formation of β-

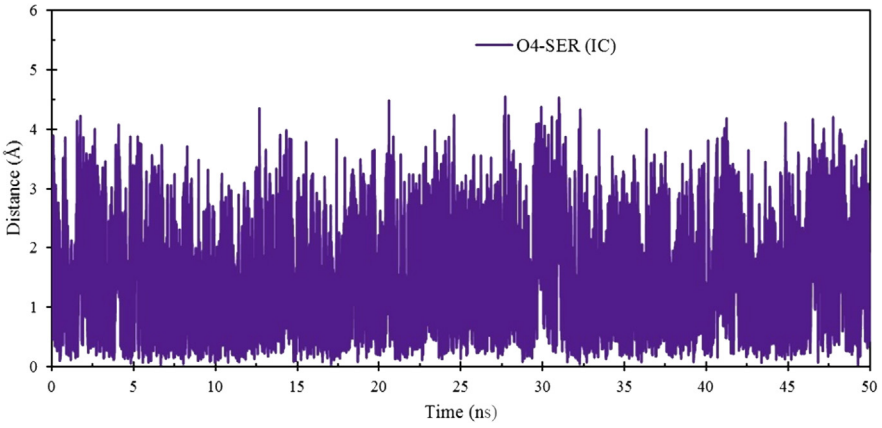

Fig. 12. The Distance between O4 of β-CD and SER in water solvent during 50 ns simulation time.

https://doi.org/10.1016/j.heliyon.2019.e01405

CD: SER IC, there are not too many fluctuations (about 0.8 Å). Thus, Fig. 12 and Fig. S6 confirms the stable complex formation between β-CD and SER.

Results were indicative of playing intermolecular H-bonds as a key role in the stability of the IC and an important non-covalent structural force (primarily electrostatic in nature) in molecular systems and also the distance between the donor and the acceptor and the angle between donor-acceptor hydrogen should be less than 0.35 nm and 30°, respectively [47]. The number of hydrogen bonds (H-bonds) between β-CD (Fig. 10a), its rims and the components of SER (Fig. 10b) during the 50 ns simulation time were computed using the CPPTRAJ module for hydrogen bonding. The results are observed in (Table 4) β-CD: SER IC is shown some hydrogen bonds between SER and β-CD, the phenolic hydrogen (H1) on the phenyl ring interacted mainly (hydrogen bond = 1223) with the O4 atom at the glycosidic bonds of β-CD and the hydrogen ($H\text{-}N^2$) on the pyrrole ring interacted chiefly with the O4 atom at the glycosidic bonds of β-CD and the hydrogens of amine ($H\text{-}N^1$) in SER interacted just with the O6 atoms at the narrow rim of β-CD. Therefore, ^{1}H-NMR, molecular docking, ICD spectroscopy and molecular dynamics study confirm the formation of IC between β-CD: SER and the location of SER ($\text{-}NH_3^+$ for side chain of pyrrole ring) in the narrow side of the β-CD cavity.

The results of MM-GBSA calculations (Table 5) confirmed the experimental data, where the formation of the most stable β-CD: SER IC was observed in ^{1}H-NMR, ICD spectroscopy and TGA, the latter algorithm is probably better optimized for

Table 4. Number of hydrogen bonds occupations for β-CD IC with SER during the 50 ns simulation time.

The kind of hydrogen binding interaction	Number of intermolecular H-bonds
	β-CD: SER IC
H^1-O (phenyl ring)…H-O^6	6
H^1-O (phenyl ring)…O^4	1223
H^1-O (phenyl ring)…H-O^3	24
H^1-O (phenyl ring)…H-O^2	65
H^2-N^2 (pyrrole ring) …H-O^6	308
H^2-N^2 (pyrrole ring) … O^4	3940
H^2-N^2 (pyrrole ring) …H-O^3	0
H^2-N^2 (pyrrole ring) …H-O^2	0
H^a-N^1 (pyrrole ring) …H-O^6	25610
H^a-N^1 (pyrrole ring) … O^4	0
H^a-N^1 (pyrrole ring) …H-O^3	0
H^a-N^1 (pyrrole ring) …H-O^2	0

[a] H^{11}, H^{12}, and H^{13} in binding with N (side chain of pyrrole ring).

https://doi.org/10.1016/j.heliyon.2019.e01405

Table 5. Energetic analysis for β-CD IC with SER using the MM-GB (PB) SA solvation models during 50 ns MD simulation.

Complex	$\Delta G_{\text{MM-GBSA}}$ (kcal/mol)	$\Delta G_{\text{MM-PBSA}}$[a] (kcal/mol)	$T\Delta S$ (kcal/mol)	ΔH (kcal/mol)
β-CD: SER	-19.22 ± 1.66	-7.13 ± 2.08	-14.86 ± 0.67	-21.99 ± 2.18

T = 298.15 K.

[a]- $\Delta G_{\text{MM-PBSA}} = T\Delta S - \Delta H$.

the analyzed systems. Additionally, the enthalpy-entropy advantage analysis suggested that the β-CD: SER complexation process tended to be enthalpy-driven and exothermic ($\Delta H < 0$) in nature. A similar phenomenon has already been observed in many experimental and theoretical studies, concerning various CD-ligand formulations [48, 49].

4. Conclusions

The results of our study represent the formation of β-CD: SER IC by the freeze-drying method in the molar ratio of 1:1 where the reaction process is enthalpy driven and exothermic representing the main role of hydrophobic interaction in the complex formation. The formation of stable β-CD: SER IC with the location of ammonium group in the pyrrole side chain of SER in the narrow side of the β-CD cavity, and the location of SER hydroxyl group in the vicinity of the wider rim of β-CD, were shown from ^{1}H-NMR and ICD spectroscopies. The results of the molecular docking, and MD calculations by using MM-PBSA, as a more accurate optimized implicit solvation model than MM-GBSA, are in agreement with the experimental results. The formation of stable IC with significant enhancement in the photostability of SER represents the great ability of β-CD for encapsulation and protection of SER that could be used in medical science for the enhancement of bioavailability, and stability of SER as an important neurotransmitter.

Declarations

Author contribution statement

Fatemeh Fateminasab: Conceived and designed the experiments; Performed the experiments; Analyzed and interpreted the data; Contributed reagents, materials, analysis tools or data; Wrote the paper.

Sergey Shityakov: Performed the experiments; Analyzed and interpreted the data.

Abdol-Khalegh Bordbar: Conceived and designed the experiments; Performed the experiments; Contributed reagents, materials, analysis tools or data.

https://doi.org/10.1016/j.heliyon.2019.e01405

Funding statement

This work was supported by the Research Council of the University of Isfahan, Isfahan, Iran.

Competing interest statement

The authors declare no conflict of interest.

Additional information

Supplementary content related to this article has been published online at https://doi.org/10.1016/j.heliyon.2019.e01405.

References

[1] S. Chaudhuri, S. Chakraborty, P.K. Sengupta, Encapsulation of serotonin in β-cyclodextrin nano-cavities: fluorescence spectroscopic and molecular modeling studies, J. Mol. Struct. 975 (2010) 160−165.

[2] K.P. Lesch, J. Waider, Serotonin in the modulation of neural plasticity and networks: implications for neurodevelopmental disorders, Neuron 76 (2012) 175−191.

[3] T. Sharp, P.J. Cowen, 5-HT and depression: is the glass half-full? Curr. Opin. Pharmacol. 11 (2011) 45−51.

[4] J. Deakin, The role of serotonin in depression and anxiety, Eur. Psychiatry 13 (Suppl 2) (1998) 57s−63s.

[5] R. Cools, K. Nakamura, N.D. Daw, Serotonin and dopamine: unifying affective, activational, and decision functions, Neuropsychopharmacology 36 (2011) 98−113.

[6] G.M. Whitford, Alzheimer ' s disease and Serotonin : a review, Neuropsychobiology 142 (1986) 133−142.

[7] M. Berger, J.A. Gray, B.L. Roth, The expanded biology of serotonin, Annu. Rev. Med. 60 (2009) 355−366.

[8] Z. Sarnyai, E.L. Sibille, C. Pavlides, R.J. Fenster, B.S. McEwen, M. Toth, Impaired hippocampal-dependent learning and functional abnormalities in the Hippocampus in mice lacking serotonin(1a) receptors, Proc. Natl. Acad. Sci. U. S. A. 97 (2000) 14731−14736.

[9] L.K. Heisler, H.-M. Chu, T.J. Brennan, J.A. Danao, P. Bajwa, L.H. Parsons, L.H. Tecott, Elevated anxiety and antidepressant-like responses in serotonin 5-HT1A receptor mutant mice, Proc. Natl. Acad. Sci. 95 (1998) 15049−15054.

[10] S. Ramboz, R. Oosting, D.A. Amara, H.F. Kung, P. Blier, M. Mendelsohn, J.J. Mann, D. Brunner, R. Hen, Serotonin receptor 1A knockout: an animal model of anxiety-related disorder, Proc. Natl. Acad. Sci. 95 (1998) 14476−14481.

[11] C.M. Portas, B. Bjorvatn, R. Ursin, Serotonin and the sleep/wake cycle: special emphasis on microdialysis studies, Prog. Neurobiol. 60 (2000) 13−35.

[12] E.M.M. Del Valle, Cyclodextrins and their uses: a review, Process Biochem. 39 (2004) 1033−1046.

[13] E. Pinho, M. Grootveld, G. Soares, M. Henriques, Cyclodextrins as encapsulation agents for plant bioactive compounds, Carbohydr. Polym. 101 (2014) 121−135.

[14] B. Gidwani, A. Vyas, A comprehensive review on cyclodextrin-based carriers for delivery of chemotherapeutic cytotoxic anticancer drugs, BioMed Res. Int. 2015 (2015) 1−15.

[15] Wasinee Khuntawee, Wolschann Peter, Thanyada Rungrotmongkol, Jirasak Wong-Ekkabut, Supot Hannongbua, Molecular dynamics simulations of the interaction of beta cyclodextrin with lipid bilayer, J. Chem. Inf. Model. 55 (2015) 1894−1902.

[16] G. Astray, C. Gonzalez-Barreiro, J.C. Mejuto, R. Rial-Otero, J. Simal-Gándara, A review on the use of cyclodextrins in foods, Food Hydrocoll. 23 (2009) 1631−1640.

[17] F. Fateminasab, A.K. Bordbar, S. Shityakov, S. Gholami, Diadzein Complexation with Unmodified Cyclodextrins: A Detailed Experimental and Theoretical Study, Elsevier B.V, 2018.

[18] K. Frömming, J. Szejtli, Cyclodextrins, in: Cyclodextrins Pharmacy. Top. Incl. Sci., Kluwer Academic Publishers, 1994, pp. 1−18.

[19] K. Uekama, F. Hirayama, T. Irie, Cyclodextrin drug carrier systems, Appl. Chem. 98 (1998) 2076.

[20] R.H. Bisby, S.W. Botchway, S. Dad, A.W. Parker, Single- and multi-photon excited fluorescence from serotonin complexed with β-cyclodextrin, Photochem. Photobiol. Sci. 5 (2006) 122−125.

https://doi.org/10.1016/j.heliyon.2019.e01405

[21] A. Abbaspour, A. Noori, A cyclodextrin host-guest recognition approach to an electrochemical sensor for simultaneous quantification of serotonin and dopamine, Biosens. Bioelectron. 26 (2011) 4674–4680.

[22] T. Higuchi, K.A. Connors, Phase-solubility techniques, Adv. Anal. Chem. Instrum. 4 (1965) 212–217.

[23] M.E. Brewster, T. Loftsson, Cyclodextrins as pharmaceutical solubilizers, Adv. Drug Deliv. Rev. 59 (2007) 645–666.

[24] G.R. Fulmer, A.J.M. Miller, N.H. Sherden, H.E. Gottlieb, A. Nudelman, B.M. Stoltz, J.E. Bercaw, K.I. Goldberg, NMR chemical shifts of trace impurities: common laboratory solvents, organics, and gases in deuterated solvents relevant to the organometallic chemist, Organometallics 29 (2010) 2176–2179.

[25] M. Kfoury, A. Lounès-Hadj Sahraoui, N. Bourdon, F. Laruelle, J. Fontaine, L. Auezova, H. Greige-Gerges, S. Fourmentin, Solubility, photostability and antifungal activity of phenylpropanoids encapsulated in cyclodextrins, Food Chem. 196 (2016) 518–525.

[26] C. Cézard, X. Trivelli, F. Aubry, F. Djedaïni Pilard, F.Y. Dupradeau, Molecular dynamics studies of native and substituted cyclodextrins in different media: 1. Charge derivation and force field performances, Phys. Chem. Chem. Phys. 13 (2011) 15103–15121.

[27] H.P. Hratchian, T.A. Keith, J. Millam, Gaussian 05 User's Reference, 2009.

[28] M.J. Frisch, G.W. Trucks, H.B. Schlegel, G.E. Scuseria, R.M.A., J.R. Cheeseman, G. Scalmani, V. Barone, B. Mennucci, G.A. Petersson, H. Nakatsuji, M. Caricato, X. Li, H.P. Hratchian, A.F. Izmaylov, J. Bloino, G.J. Zheng, J.L. Sonnenberg, M. Hada, M. Ehara, M. Toyota, K. Fukuda, R. Hasegawa, J. Ishida, Y. Nakajima, T. Honda, O. Kitao, J.E. Nakai, H. Vreven, T. Montgomery, J.A. Peralta Jr., M. Ogliaro, F. Bearpark, E. Heyd, J.J. Brothers, V.N. Kudin, K.N. Staroverov, K. Kobayashi, R. Normand, J. Raghavachari, J.C. Rendell, A. Burant, S.S. Iyengar, J. Tomasi, M. Cossi, N. Rega, N.J. Millam, V. Klene, M. Knox, J.E. Cross, J.B. Bakken, J. Adamo, C. Jaramillo, C. Gomperts, R. Stratmann, R.E. Yazyev, O. Austin, A.J. Cammi, R. Pomelli, R.L. Ochterski, J.W. Martin, V.G. Morokuma, K. Zakrzewski, G.A. Voth, P. Salvador, J.J. Dannenberg, S. Dapprich, A.D. Daniels, Ö. Farkas, J.B. Foresman, J.V. Ortiz, J. Cioslowski, D.J. Fox, Gaussian 09 User's Reference, Gaussian, Inc, Wallingford CT, 2009. http://gaussian.com/references/.

https://doi.org/10.1016/j.heliyon.2019.e01405

[29] G.M. Morris, D.S. Goodsell, R.S. Halliday, R. Huey, W.E. Hart, R.K. Belew, A.J. Olson, AutoDock-related material automated docking using a lamarckian genetic algorithm and an empirical binding free energy function, Comput. Chem. J. Comput. Chem. 19 (1998) 1639−1662.

[30] D.A. Case, T. Darden, T.E. Cheatham, C. Simmerling, J. Wang, R.E. Duke, R. Luo, R.C. Walker, W. Zhang, K.M. Merz, B.P. Roberts, S. Hayik, A. Roitberg, G. Seabra, J. Swails, A.W. Götz, I. Kolossváry, K.F. Wong, F. Paesani, J. Vanicek, R.M. Wolf, J. Liu, X. Wu, S.R. Brozell, T. Steinbrecher, H. Gohlke, Q. Cai, X. Ye, J. Wang, M.-J. Hsieh, G. Cui, D.R. Roe, D.H. Mathews, M.G. Seetin, R. Salomon-Ferrer, C. Sagui, V. Babin, T. Luchko, S. Gusarov, A. Kovalenko, P.A. Kollman, Amber 12 Reference Manual Principal Contributors to the Current Codes, 2012.

[31] J. Wang, R.M. Wolf, J.W. Caldwell, P.A. Kollman, D.A. Case, Development and testing of a general amber force field, J. Comput. Chem. 25 (2004) 1157−1174.

[32] S. Shityakov, R.E. Salmas, S. Durdagi, E. Salvador, K. Pápai, M.J. Yáñez-Gascón, H. Pérez-Sánchez, I. Puskás, N. Roewer, C. Förster, J.A. Broscheit, Characterization, in vivo evaluation, and molecular modeling of different propofol-cyclodextrin complexes to assess their drug delivery potential at the blood-brain barrier level, J. Chem. Inf. Model. 56 (2016) 1914−1922.

[33] S. Shityakov, R.E. Salmas, S. Durdagi, N. Roewer, C. Förster, J. Broscheit, Solubility profiles, hydration and desolvation of curcumin complexed with γ-cyclodextrin and hydroxypropyl-γ-cyclodextrin, J. Mol. Struct. 1134 (2017) 91−98.

[34] H. Zhang, T. Tan, W. Feng, D. Van Der Spoel, D. van der Spoel, Molecular recognition in different environments: β-cyclodextrin dimer formation in organic solvents, J. Phys. Chem. B 116 (2012) 12684−12693.

[35] J. Wang, P. Cieplak, P.A. Kollman, How well does a restrained electrostatic potential (RESP) model perform in calculating conformational energies of organic and biological molecules? J. Comput. Chem. 21 (2000) 1049−1074.

[36] C. Cézard, X. Trivelli, F. Aubry, F. Djedaïni-Pilard, F.-Y.Y. Dupradeau, F. Djedaïni Pilard, F.-Y.Y. Dupradeau, Molecular dynamics dtudies of native and substituted cyclodextrins in different media: 1. Charge derivation and force field performances, Phys. Chem. Chem. Phys. 13 (2011) 15103−15121.

[37] I. Mourtzinos, N. Kalogeropoulos, S.E. Papadakis, K. Konstantinou, V.T. Karathanos, Encapsulation of nutraceutical monoterpenes in β-cyclodextrin and modified starch, J. Food Sci. 73 (2008) 89−94.

https://doi.org/10.1016/j.heliyon.2019.e01405

[38] N. Roik, L. Belyakova, IR Spectroscopy, X-ray Diffraction and Thermal Analysis studies of Solid "β-Cyclodextrin-para-Aminobenzoic Acid" Inclusion Complex, Phys. Chem. Solid State. 1 (2011) 168−173. http://www.pu.if.ua/inst/phys_che/start/pcss/vol12/1201-26.pdf.

[39] M.L. Alonso, E. Sebasti??n, L.S. Felices, P. Vitoria, R.M. Alonso, Structure of the β-cyclodextrin: acetamiprid insecticide inclusion complex in solution and solid state, J. Incl. Phenom. Macrocycl. Chem. 86 (2016) 103−110.

[40] R.L. Abarca, F.J. Rodríguez, A. Guarda, M.J. Galotto, J.E. Bruna, E. Bruna, Characterization of beta-cyclodextrin inclusion complexes containing an essential oil component, Food Chem. 196 (2015) 968−975.

[41] K. Harata, Hisashi Uedaira, The circular dichroism spectra of the β-cyclodextrin complex with naphthalene derivatives, Bull. Chem. Soc. Jpn. 48 (1975) 375−378.

[42] D.R. Roe, T.E. Cheatham III, PTRAJ and CPPTRAJ: software for processing and analysis of molecular synamics trajectory data, J. Chem. Theory Comput. 9 (2013) 3084−3095.

[43] B. Nutho, W. Khuntawee, C. Rungnim, P. Pongsawasdi, P. Wolschann, A. Karpfen, N. Kungwan, T. Rungrotmongkol, Binding mode and free energy prediction of fisetin/β-cyclodextrin inclusion complexes, Beilstein J. Org. Chem. 10 (2014) 2789−2799.

[44] W. Cai, T. Sun, C. Chipot, Can the anomalous aqueous solubility of β-cyclodextrin be explained by its hydration free energy alone? Phys. Chem. Chem. Phys. 10 (2008) 3236−3243.

[45] C. Huang, C. Li, P.Y.K. Choi, K. Nandakumar, L.W. Kostiuk, Effect of cut-off distance used in molecular dynamics simulations on fluid properties, Mol. Simul. 36 (2010) 856−864.

[46] A. Figueiras, J.M.G. Sarraguc, R.A. Carvalho, A.A.C.C. Pais, F.J.B. Veiga, Interaction of omeprazole with a methylated derivative of β-cyclodextrin: phase solubility, NMR spectroscopy and molecular simulation, Pharm. Res. 24 (2007) 377−389.

[47] P.C. Nair, J.O. Miners, Molecular dynamics simulations: from structure function relationships to drug discovery, Silico Pharmacol. 2 (2014) 1−4.

[48] H.E. Grandelli, B. Stickle, A. Whittington, E. Kiran, Inclusion complex formation of β-cyclodextrin and naproxen: a study on exothermic complex formation by differential scanning calorimetry, J. Incl. Phenom. Macrocycl. Chem. 77 (2013) 269−277.

https://doi.org/10.1016/j.heliyon.2019.e01405

[49] J.E.H. Köhler, N. Grczelschak-mick, J. Erika, H. Köhler, N. Grczelschak-mick, The β-cyclodextrin/benzene complex and its hydrogen bonds− a theoretical study using molecular dynamics, quantum mechanics and COSMO-RS, Beilstein J. Org. Chem. 9 (2013) 118−134.

https://doi.org/10.1016/j.heliyon.2019.e01405